

T. Ueda
Research Associate.

A. Hosokawa
Research Assistant.

Department of Mechanical Engineering,
Faculty of Engineering Science,
Osaka University,
Toyonaka 560,
Japan

A. Yamamoto
Professor,
Department of Industrial Engineering,
Faculty of Science and Technology,
Kinki University,
Kowakae 3-4-1, Higashiosaka 577,
Japan

Measurement of Grinding Temperature Using Infrared Radiation Pyrometer With Optical Fiber

The heat pulses produced by cutting grains in a workpiece were measured using an infrared radiation pyrometer connected by means of an optical fiber. The results obtained were compared with those from a thermocouple to investigate the effect of differences in response speed on the output. The I.R.P., using an InAs cell as a detector which has a response time in the order of μs , can detect heat pulses with great accuracy and its signal trace versus time has many sharp peaks. The thermocouple formed by spot welding is inferior in response speed, and less accurate in registering heat pulses.

1 Introduction

The grinding temperature in the surface layer of a workpiece is a significant factor in investigation of a grinding mechanism. Exact measurement is very difficult because the temperature gradients are very steep with respect to both time and space.

The thermocouple, the typical thermometer of the contact type, has advantages for measuring the inner temperature of an object because it can be implanted in the object. Littmann [1], Takazawa [2], and Peklenik [3] used the thermocouple technique to measure the grinding temperature in a workpiece. However, correct calibration of the thermocouple is difficult at high temperatures, and it cannot respond to rapid changes of temperature. Moreover, the influence of the response time on measurement accuracy has not been yet investigated, since there have been no other suitable methods of temperature measurement to make comparison with this method possible.

The infrared radiation pyrometer (I.R.P.), the noncontact type of thermometer, has many advantages: it can respond to rapid changes of temperature, and enables us to easily measure high temperatures without disturbing heat distribution. Mayer and Shaw [4] obtained the temperature of a freshly ground surface by measuring the infrared radiation emitted from it. Kops and Shaw [5, 6] measured qualitatively the infrared radiation emitted from wheel and chips using various infrared radiation measurement techniques. However, I.R.P. can be used only to measure the surface temperature of an object, and it is necessary to know its emissivity to do a quantitative measurement. Moreover, we have to use a microscope to measure the temperature of a very small area and in this case the setting distance is very short.

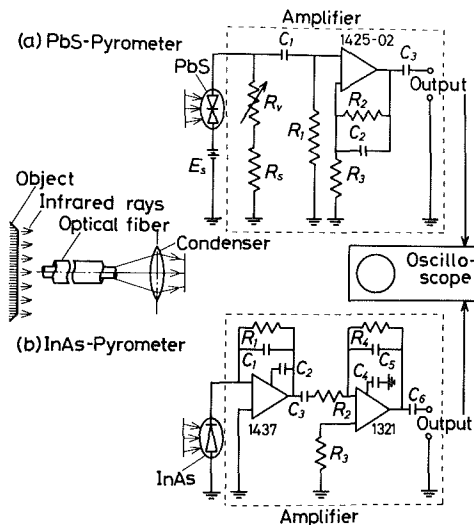


Fig. 1 Systems of PbS-I.R.P. and InAs-I.R.P.

Recently, the authors made a new type of infrared radiation pyrometer in which an optical fiber accepts the infrared flux radiated from the object and transmits it to an infrared detector InAs cell. This I.R.P. is suitable for measuring the temperature of a very small object whose temperature changes rapidly. Besides, the flexibility of the optical fiber makes it possible to measure the inner temperature of the object by drilling a microscopically fine hole in it and inserting the fiber. Using this pyrometer, we succeeded in measuring quantitatively the temperature of cutting grains on a grinding wheel just after cutting [7].

In this study, the heat pulses produced by cutting grains in the surface layer of a workpiece are measured by this new

Contributed by the Production Engineering Division for presentation at the Winter Annual Meeting, Anaheim, California, December 7-12, 1986, of THE AMERICAN SOCIETY OF MECHANICAL ENGINEERS. Manuscript received at ASME Headquarters, July 1, 1986. Paper No. 86-WA/Prod-6.

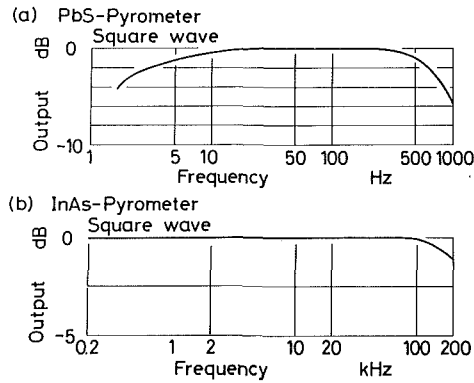


Fig. 2 Frequency characteristics of PbS-I.R.P. and InAs-I.R.P.

method using InAs and PbS cells as IR-detectors. The results obtained are compared with those of the thermocouple in order to investigate the influence of the response speed on output and to estimate the response speed of the thermocouple. In addition, the effect of the setting location of the fiber on measurement accuracy is investigated, both theoretically and experimentally.

2 Pyrometer

2.1 System and Frequency Response. Schematic illustrations of the infrared radiation pyrometer using InAs and PbS cells as detectors are shown in Fig. 1. The infrared rays radiated from the object are accepted and transmitted by the fiber, and led to the detector through a condenser. Infrared energy is converted to an electric signal by the detector and is then amplified and observed on an oscilloscope screen.

The response speed of the pyrometer is closely related to measurement accuracy. Figure 2(a), which represents the frequency characteristics of PbS-I.R.P., shows a flat response for pulses of infrared rays in the range 10 Hz–400 Hz. Figure 2(b), which represents the characteristics of the amplifier of InAs-I.R.P., shows a flat response for a square wave of 0.2 kHz–100 kHz. (The time constant of the InAs cell is approximately 1 μ s.) As the signal to be measured is a pulse of about several tens μ s, the InAs pyrometer can be used with a good degree of accuracy.

2.2 Influence of Setting Location of Fiber on Measurement Accuracy. The infrared rays radiated from an object are accepted and transmitted by a fiber. Therefore, in using this pyrometer it is necessary to carefully examine the influence on measurement accuracy of the setting location of the fiber face. In this section, the influence of the setting location of the fiber on the target area and the energy accepted will be investigated both theoretically and experimentally.

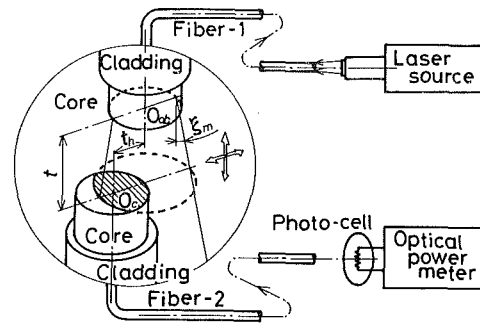


Fig. 3 Apparatus for measuring optical power accepted by fiber

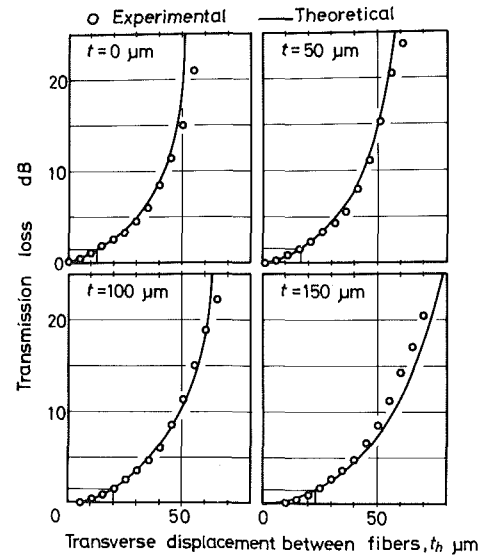


Fig. 4 Influence of transverse displacement between optical fibers on transmission loss

2.2.1 Target Area. The theoretical proposition for the target area is contained in another paper by the present authors [7]. When a fiber is placed vertically at a distance of t from the object, the target area S_t of this pyrometer is expressed by

$$S_t = \left(t \tan \xi_m + \frac{d}{2} \right)^2 \pi \quad (1)$$

where d is the core diameter and ξ_m is the acceptance angle. This equation is derived assuming that all rays which are incident on the face of fiber with an angle less than the acceptance angle ξ_m can be transmitted, and that the distribution of the energy intensity on the cross section of the core is uniform. An experiment was conducted in order to examine these assumptions.

Nomenclature

a = wheel depth of cut, μ m
 d = diameter of fiber core, μ m
 e_λ = radiant energy from df accepted by fiber, W
 de_λ = elementary energy emitted from df incident on dF' , W
 E_λ = total radiant energy transmitted by fiber, W
 df = elementary area in measuring area, μ m²
 F' = incidence area in fiber face emitted from df , μ m²

dF' = elementary area in fiber face, μ m²
 $J_{\lambda n}$ = normal spectral radiant intensity of blackbody, W/(sr·m²· μ m)
 r_f = $t \tan \xi_m$, μ m
 R = distance between df and dF' , μ m
 S_c = area of core, μ m² ($= \pi d^2/4$)
 S_t = target area of pyrometer, μ m²
 t = distance between object and incidence face of fiber, μ m

t_h = transverse displacement between optical fibers, μ m
 v = workpiece speed, m/min
 V = peripheral speed of wheel, m/min
 λ = wavelength, μ m
 λ_2 = upper limit wavelength of measurable range in pyrometer, μ m
 ξ = angle of incidence, rad
 ξ_m = acceptance angle, rad
 $d\omega$ = solid angle, sr

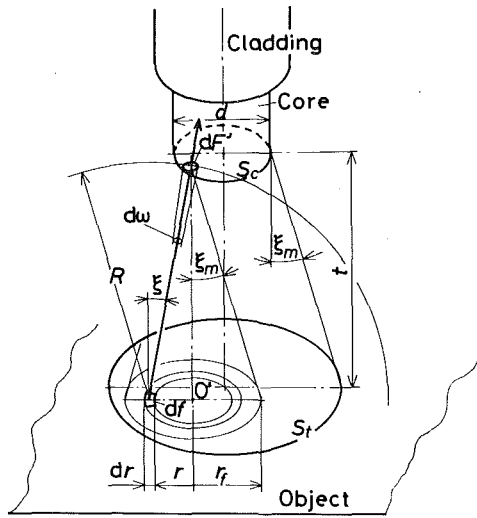


Fig. 5 Illustration of energy accepted at incidence face of optical fiber

tions. As shown in Fig. 3, radiation from the laser source (wavelength $\lambda_s = 0.6328 \mu\text{m}$) is emitted uniformly from the face of Fiber-1 onto the face of Fiber-2. The emission face is treated as the object. The laser power from the emission face of Fiber-1 is accepted by Fiber-2 placed at a distance of t and transmitted through it to the optical power meter, with various transverse displacements t_h between optical fibers.

Experimental and theoretical results are compared in Fig. 4. The theoretical results are calculated on the same assumptions mentioned above—that is, the energy intensity emitted from Fiber-1 is distributed uniformly over its core face, and all energy accepted by Fiber-2 with an angle less than the acceptance angle ξ_m (hatched area shown in Fig. 3), can be transmitted without any losses.¹ As the theoretical results agree with the experimental results at various distances of t , the reasonableness of these two assumptions has been confirmed. Consequently, we can use equation (1) to calculate the target area of this pyrometer.

2.2.2 Energy Accepted. In Fig. 5, a fiber is placed vertically at a distance of t from an object. The most convenient case is when the object is larger than the target area. The following theory is developed on the assumptions that the object has a blackbody surface at a uniform temperature, and that there are no losses at all. The energy element de_λ emitted from df into a solid angle $d\omega$ is expressed by the following equation,

$$de_\lambda = J_{\lambda n} d\lambda \cos \xi df d\omega \quad (2)$$

where $J_{\lambda n}$ is the normal spectral radiant intensity. Substituting the equation $d\omega = dF' \cos \xi / R^2 = dF' \cos^3 \xi / t^2$ to equation (2),

$$de_\lambda = J_{\lambda n} d\lambda \cos^4 \xi df \frac{1}{t^2} dF' \quad (3)$$

where dF' is the element of area in the fiber face expressed by a solid angle $d\omega$. Here, the element of area, df , now indicates a circular ring of radius r with center O' , $df = 2\pi r dr$,

$$de_\lambda = J_{\lambda n} d\lambda 2\pi dF' \frac{r \cos^4 \xi}{t^2} dr \quad (4)$$

Integrating this equation in the region $0 \leq r \leq r_f (= t \tan \xi_m)$,

$$e_\lambda = J_{\lambda n} d\lambda \frac{\pi}{2} dF' [1 - \cos(2\xi_m)] \quad (5)$$

¹The theoretical curves were obtained by using equation (7) in the present authors' paper [7].

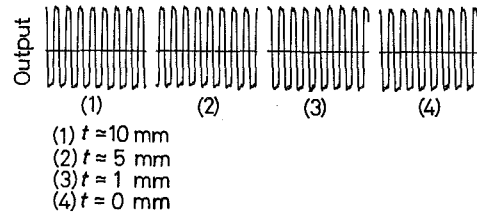


Fig. 6 Influence of distance between object and incidence face of optical fiber on sensitivity of I.R.P.

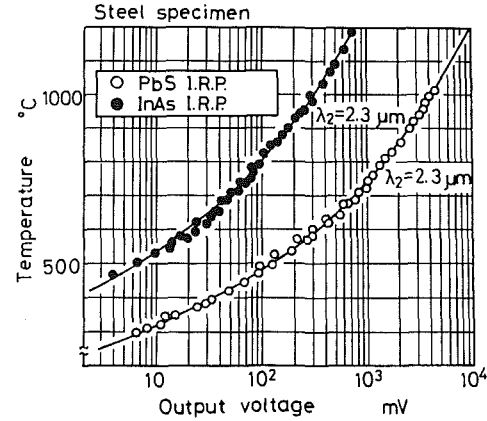


Fig. 7 Calibration curves of PbS-I.R.P. and InAs-I.R.P.

Therefore, the total radiant energy transmitted E_λ is obtained by integrating equation (5) over the whole area of the core S_c ,

$$\begin{aligned} E_\lambda &= J_{\lambda n} d\lambda \frac{\pi^2 d^2}{8} [1 - \cos(2\xi_m)] \\ &= J_{\lambda n} d\lambda \pi S_c (NA)^2 \end{aligned} \quad (6)$$

where NA is the numerical aperture of the fiber and $NA = \sin \xi_m$ in the air. Equation (6) suggests that E_λ does not depend on t but on S_c and NA , which is the same result obtained in the authors' previous paper [7]. Consequently, the energy accepted by this pyrometer does not depend on the distance between the fiber and the object when the object is larger than the target area.

Let us examine these results experimentally. Figure 6 shows the output of InAs-I.R.P. for a large specimen kept at constant temperature, when the distance of t between the specimen and the incidence face of optical fiber is changed. The infrared rays radiated from the object are measured by I.R.P. after they are chopped, so that the amplitude of the output waves represents the output voltage of the pyrometer. As is evident from Fig. 6, the distance of t has no effect on the energy accepted, that is, on the sensitivity of the pyrometer. Consequently, the propriety of equation (6) has been confirmed experimentally.

3 Calibration

The calibration curves of the two pyrometer types, shown in Fig. 7, are obtained by sighting on radiating surfaces of known uniform temperature. The temperature of a carbon steel target was checked by a C-A used thermocouple. The characteristics of the optical fiber used are shown in Table 1. The curves in Fig. 7 stand for the relative sensitivities, which are calculated from the spectral transmittance of the fiber and condenser and from the spectral sensitivity of the infrared detector (as mentioned in the previous paper [7]). As can be seen, the experimental points coincide well with the calculated curves.

4 Measurement of Grinding Temperature

4.1 Experiment. Surface grinding was carried out at a constant wheel depth of cut. The experimental arrangement is illustrated schematically in Fig. 8 and the experimental conditions are summarized in Table 2. With the infrared radiation pyrometers using InAs and PbS cells as detectors, the optical fiber is inserted into a small hole (its diameter is approximately 0.4 mm) which extends nearly to the ground surface. If there is a small distance between the incidence face of the fiber and the bottom of the hole, this does not influence the measurement accuracy because the area of the bottom of the hole is larger than the area of the fiber. The fiber can accept the infrared rays radiated from the bottom, when the grinding wheel passes above it. One pass grinding was continued until the bottom of the hole was ground through.

The grinding temperature is also measured by means of a thermocouple formed by spot welding a constantan wire (0.1 mm diameter) at the bottom of a small hole (0.4 mm

Table 1 Characteristics of fiber

Core diameter $d = 50 \mu\text{m}$
Numerical aperture $NA = 0.23$
Relative index difference $\Delta = 1.15 \%$
Acceptance angle $2\xi_m = 26.2 \text{ deg}$

Table 2 Summary of experimental conditions

Grinding conditions
Number of revolutions of wheel = 1800 rpm
Peripheral speed of wheel $V = 1696 \sim 1713 \text{ m/min}$
Workpiece speed $v = 10 \text{ m/min}$
Wheel depth of cut $a = 20 \mu\text{m}$
Up grinding
Grinding wheel
A36K7VC(3)B, $(300 \sim 303) \times 30 \times 127 [\text{mm}]$
$V_p = 40.0 \%$, $V_G = 49.1 \%$, $V_B = 10.9 \%$
Workpiece
0.55 % carbon steel, Hv 200
Width = 6 mm
Length = 52 mm

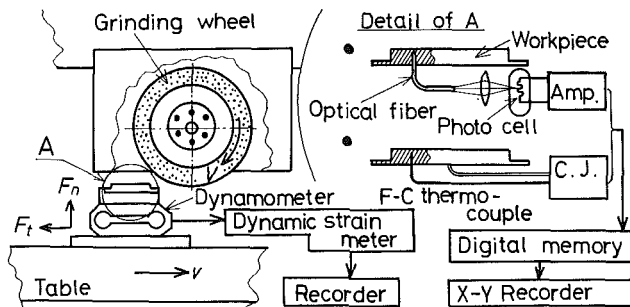


Fig. 8 Schematic illustration of experimental set-up

diameter). In addition, the temperature of cutting points is measured using a thermocouple technique devised by Peklenik [3], in which a fine constantan wire insulated with mica is inserted into a workpiece. Metal chips produced during grinding by abrasive grains close the circuit between the surface of the constantan wire and the workpiece. The output voltage is stored in a digital memory (sampling time is $2 \mu\text{s}$) and reproduced on an X-Y recorder.

4.2 Output Wave. Figure 9 is the comparison of output waves measured with three kinds of pyrometers. The signals show the grinding temperature histories for various depths below the ground surface. One horizontal division represents 1 ms and is equivalent to 0.15 mm along the surface of the workpiece. Since the thermocouple formed by spot welding is inferior in response time, it cannot detect the heat pulses and its signal trace versus time is observed as a smooth curve without any peaks.

The PbS-I.R.P., which has a response time of $200 \mu\text{s}$, can detect some heat pulses at $20 \mu\text{m}$ depth below the ground surface, but the number of pulses is small and their shape is not clearly defined. This indicates that the response speed of this pyrometer is also insufficient for the detection of heat pulses in grinding. Estimating from these results, the thermocouple should be used to measure the pulse of few millisecond width or more.

However, the InAs-I.R.P., which has a response time in the order of μs , can detect some pulses even at $40 \mu\text{m}$ depth below the ground surface, and many sharp pulses at $20 \mu\text{m}$ depth. The trace also indicates that there are great changes of temperature ($100^\circ\text{C} \sim 200^\circ\text{C}$) within few hundred μs width.

From these results, it is clear that we must pay close attention to the response speed of a pyrometer used in measuring

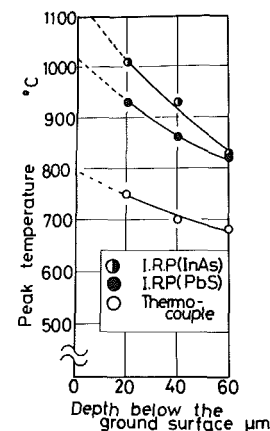


Fig. 10 Comparison of peak temperatures in surface layer of workpiece

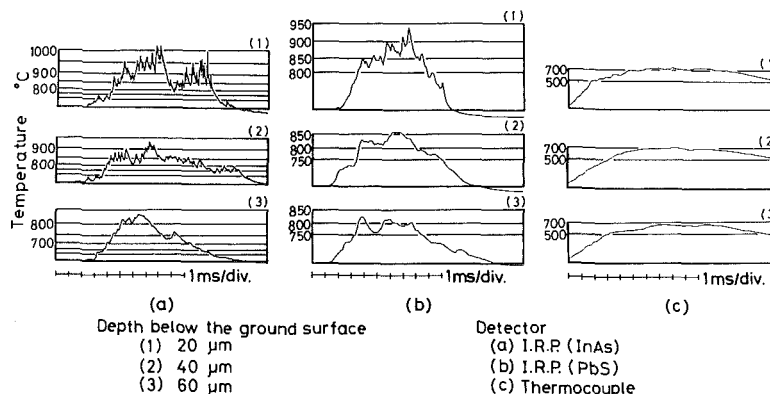


Fig. 9 Comparison of output waves measured with three kinds of pyrometers

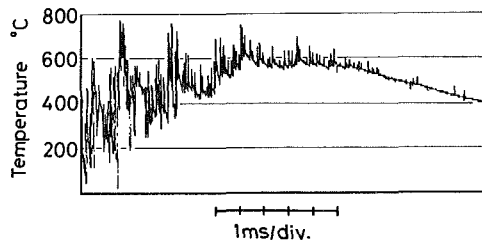


Fig. 11 Output wave measured with thermocouple technique devised by Peklenik

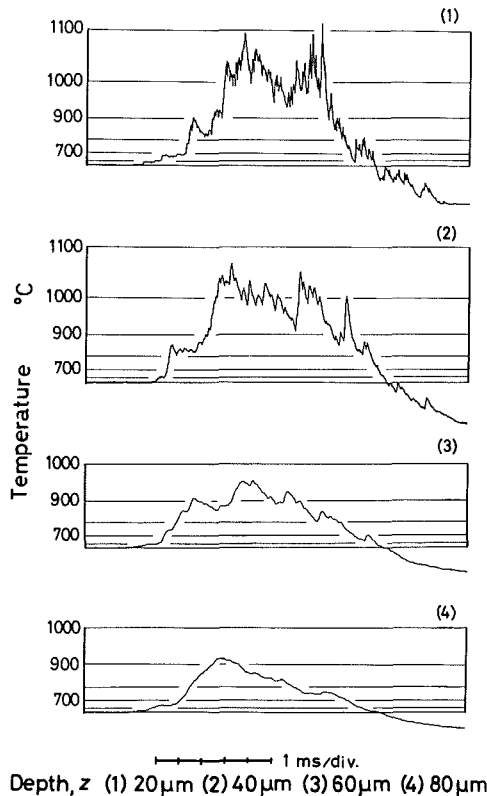


Fig. 12 Variation of temperature in workpiece measured with InAs-I.R.P. in wet grinding

grinding temperature. (It is possible to measure the grinding temperature in a workpiece more precisely by using a fiber with a finer core and drilling a smaller hole in the workpiece.)

4.3 Grinding Temperature in the Workpiece. Figure 10 compares the peak temperature in a workpiece measured with these three kinds of pyrometers. These data are obtained by reading the maximum peak temperature at each depth below the ground surface indicated in Fig. 9. As is obvious from Fig. 10, the pyrometer of higher response speed obtains the higher temperature. Extrapolation of these data indicates that the maximum surface temperature using InAs-I.R.P. is higher than 1100°C .

Figure 11 shows the output wave measured with the thermocouple technique devised by Peklenik. It has always been considered that this is the most suitable method to measure the surface temperature of a workpiece. However, the maximum peak temperature is 800°C at most, as Fig. 11 shows. This result, in which the trace is not broken but is a continuous curve with many peaks, indicates that a circuit is made between the constant wire and the workpiece in the large region caused by their plastic deformation, and many peaks are made when the cutting grits pass through this region – that

is to say, the region of high temperature made by cutting grits in the hot junction is smaller than that of the lower temperature caused by plastic deformation. When the temperature in the hot junction is not uniform, the output voltage produced by the thermocouple approximately indicates the mean temperature of the hot junction. Consequently, although the change of temperature can be detected with this method, the response to it is not accurate.

4.4 Effect of Grinding Fluid. Figure 12 shows the variation of temperature in the surface layer measured with InAs-I.R.P. in wet grinding. Grinding fluid (soluble oil, 1:50 in water) is supplied to the grinding zone from the tangential direction of the wheel. Comparing these results with those in Fig. 9(a), there are few differences with respect to the shape of the output waves and the maximum peak temperature. However, the temperature of the workpiece decreases more quickly after grinding with fluid. Consequently, the grinding fluid has the effect of taking away the heat from the workpiece and reducing its mean temperature, but it cannot reach the cutting points in the grinding zone and prevent the generation of heat.

5 Conclusions

The properties of a new temperature measuring method, in which an optical fiber accepts the infrared rays radiated from an object and transmits it to an infrared detector, were confirmed experimentally. Applying this pyrometer with InAs and PbS cells to surface grinding, the heat pulses produced by the cutting grains in a workpiece were measured. The results obtained were compared with those of the thermocouple to investigate the influence of response speeds on the output. Since the thermocouple formed by spot welding is inferior in response speed, it cannot detect the heat pulses and its signal trace versus time is observed as a smooth curve without any peaks. The trace obtained by InAs-I.R.P., which has the response time in the order of μs , has many sharp peaks, because it can faithfully respond to the rapid changes of temperature. The highest surface temperature, which is estimated by extrapolating peak temperatures in the workpiece, is obtained using this pyrometer. The thermocouple technique devised by Peklenik can also detect the change of temperature, but it is impossible for it to respond accurately. Grinding fluid has the effect of taking away the heat from the workpiece and decreasing its mean temperature, but it cannot reach the cutting points in the grinding zone and prevent the generation of heat.

Acknowledgment

The authors are indebted to The Fujikura Cable Works Co., Ltd. for providing the optical fibers.

References

- 1 Littmann, W. E., and Wulff, J., "The Influence of the Grinding Process on the Structure of Hardened Steel," *Trans. ASM*, Vol. 47, 1955, pp. 692-714.
- 2 Takazawa, K., "Effects of Grinding Variables on the Surface Structure of Hardened Steel," *Bull. Japan Soc. of Precision Engineering*, Vol. 2, No. 1, Apr. 1966, pp. 14-19.
- 3 Peklenik, J., "Der Mechanismus des Schleifens und die Überschliffzahl," *Industrie-Anzeiger*, Vol. 80, No. 1, Jan. 1958, pp. 10-17.
- 4 Mayer, J. E., Jr., and Shaw, M. C., "Grinding Temperatures," *Journal of American Society of Lubrication Engineers*, Vol. 13, 1957, pp. 21-27.
- 5 Kops, L., and Shaw, M. C., "Thermal Radiation in Surface Grinding," *Annals of the CIRP*, Vol. 31, No. 1, 1982, pp. 211-214.
- 6 Kops, L., and Shaw, M. C., "Application of Infrared Radiation Measurement in Grinding Studies," *Proc. NAMRC-XI, SME Mfg. Eng. Trans. J.*, 1983, pp. 390-396.
- 7 Ueda, T., Hosokawa, A., and Yamamoto, A., "Studies on Temperature of Abrasive Grains in Grinding—Application of Infrared Radiation Pyrometer," *ASME JOURNAL OF ENGINEERING FOR INDUSTRY*, Vol. 107, No. 2, 1985, pp. 127-133.